

## Thermo-mechanical study of artificial aggregates-based concrete derived from the Thicky clays (Senegal)

*Aida GAYE, Prince Momar GUEYE, Dame KEINDE, and Ndèye Awa SENE*

Département of Civil Engineering, Cheikh Anta Diop University, Ecole Supérieure Polytechnique, Dakar, Senegal

Copyright © 2018 ISSR Journals. This is an open access article distributed under the *Creative Commons Attribution License*, which permits unrestricted use, distribution, and reproduction in any medium, provided the original work is properly cited.

**ABSTRACT:** Senegal has at its disposal a lot of mineral deposits among which the clay. This material is usable mostly in the production of pottery, the manufacture of bricks or tiles. Nevertheless, the increasing use of some natural aggregates in construction, more accurately gravels like basalt as well as limestone, could expose them to depletion. It is within this framework that our research, which is about the thermo-mechanical study of clay gravel-based concrete, has been developed. It consists of replacing common gravels with expanded clay aggregates. To that end, we have tested the clay of Thicky, which the SOFAMAC factory uses to manufacture its building materials. We used different methods to get expanded clay aggregates at different temperatures. We also did the characterization of these expanded clay aggregate as well as that of clay concrete. The results obtained from the gravels have been compared with those from common concretes. They indicate that the use of these gravels bring satisfactory results when they undergo an adequate transformation.

**KEYWORDS:** Thermo-mechanic, study, artificial aggregates, clay of Thicky, Senegal.

### 1 INTRODUCTION

Clay has been one of the basic materials used in house building since antiquity. It is an easy-to-use, resistant and waterproof material when it is well kneaded with water. Furthermore, it makes possible a good thermal insulation and is fire resistant. All these properties have then allowed its use in the past, particularly in the building sector. It can be produced artificially using raw materials like clay, slate, schist, slag, sintered fly ash, expanded polystyrene [1-3].

The mechanic properties of lightweight aggregate-based concretes depend heavily, in addition to the quality of the cement matrix, on the volume and characteristics of lightweight aggregates [5-6].

It is of a paramount importance for this fast-growing sector to streamline the structure, minimize energy costs and ensure comfort. So, it becomes essential to find available (local) materials capable of meeting the specifications as well as being competitive.

In Senegal, the abundant supply of clay has made us want to use this natural or artificial resource in construction and to profit from its potentials. Thus, we have proposed the substitution of common gravels i.e. basalt and limestone by the expanded clay of the concrete, which permits us to obtain lightweight concrete. For this purpose, we need to do the characterization and the thermo-mechanical study of the clay granule-based concrete.

Though, clay has always been considered as a pollutant, hence the tests to determine the cleanliness of the sand - sand equivalence or methylene blue test- which ranked them among unwanted materials for concrete. We will do different types of tests on clay products and check if they can improve the concrete.

This article will first deal with the characterization of aggregates and then the thermo-mechanical characterization of the clay gravel-based concrete.

## 2 PROCEDURE TO OBTAIN ARTIFICIAL AGGREGATES

The tested clay comes from Thick, more accurately from the SOFAMAC factory quarries, under the banner of MATEC. This locality is situated in the DIASS area in SENEGAL. This clay is extracted deep in the soil that is made up of laterite on the first layer, followed by yellow clay and finally by gray clay. That gray clay is the one we will use in our study.

Clay is the artificial granule that is tested. They are artificial because they are constituted from the diverse physical and chemical transformations of the natural aggregates or others (residues or wastes from blast-furnace). In our case, the clay is obtained through physical and thermal processing.

We went through different processes to obtain the needed clay aggregates for our study. These processes include the extraction, the grinding, the winding and finally the firing. For the extraction, we collected a stock from the factory.

### 2.1 GRINDING PROCESS

We used the Los Angeles machine for the grinding (Figure 1) to get clay powder.



*Fig. 1. The Los Angeles machine*

This machine has 11 heavy steel balls (Figure 2). It does a predetermined number of rotations around itself. For the grinding, the default setting is at 500 rotations. When the machine is running, the clash between the material particles and the balls splits them up, and as the machine is rotating around itself, particles become smaller and smaller. A 1.25mm-sieve (Figure 3) helps to collect the clay powder.



*Fig. 2. steel balls*



*Fig.3. sieve*

### 2.2 THE WINDING PROCESS

This stage consists of creating clay aggregates from the powder collected after sieving the clay (figure 5). The cement mixer has been used for that (figure 4). An amount of clay powder has been put in the cement mixer. While the machine is running, water equivalent to 17% of that mass is continuously poured inside it. The mixing takes 10 to 15 minutes with regular breaks going up to 1 minute to allow the scraping of the cement mixer, thus avoiding that particles get attached to the wall of the machine. The 17% represent the plasticity line stated in paragraph 3- beyond this quantity of water that should be added, the end product will be liquid.



*Fig. 4. Cement mixer*



*Fig.5. Clay aggregates*

### 2.3 FIRING

The unfired clay we get after the winding with the cement mixer is inserted into a furnace in the metallic laboratory of the Centre d'Entreprenariat et de Développement Technique (CFDT/ Entrepreneurship and technical development center) known as G15, located in Colobane. The oven is composed of a tube that allows the transmission of the heat, but also of springs on the two edges which become red when the heat reaches the inside of the oven properly. Concerning the firing, different temperatures were used in order to assess the most suitable one for a better lightweight aggregate. Two temperatures were selected: the first at 860°C and the second at 1100°C. The fired clay becomes red as a result of the heat, which means that the higher the temperature, the more the color of the clay turns brick-red. The samples we obtained are presented in figures 6 and 7.



*Fig. 6. Clay-based artificial gravels 8/16 fired at 860°C*



*Fig. 7. Clay-based artificial gravels 8/16 fired at 1100°C*

In the end, we got two types of clay-based artificial gravels: clay aggregates fired at 1100°C and those fired at 860°C.

### 3 CHARACTERIZATION OF THE CLAY OF THICKY

The particle size grading achieved by sedimentation, which consists of applying the Stock law on particles suspended in a fluid, has given 4 medium-sized populations centered at 3,5µm, 9µm, 35 µm and 80µm. Besides, 99% of the material is below 80µm. We can then assert that this clay is composed of fine particles (figure below).

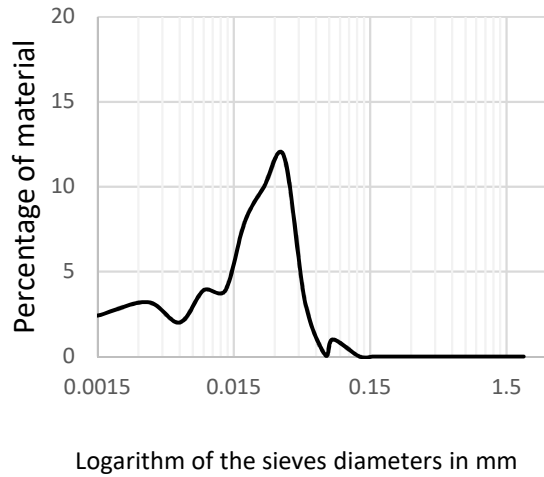


**Fig. 8. Granulometric distribution of the clay of Thicky**

The material’s plasticity index is done using the Atterberg limits; the liquidity limit is determined thanks to the Casagrande apparatus and the plastic limit by the method of rollers. The difference between the two limits gives the plasticity index. The results are in the following table:

**Table 1. Limits of the water content and plasticity index**

	LL	LP	IP
Clay from Thicky	70,1	17,1	53

The chemical analysis of the materials is carried out by ICP (Sectro Plasma Iris). It has given the basic composition of our material (Table 2). Actually, this material is essentially made of silica and alumina. These two oxides represent about 80% of the total clay portion.

The mineral components are identified by x-ray diffraction (DRX) at the x-ray laboratory of FST UCAD. The machine is a Phillips X’Pert, Cu $\alpha$  radiation. Results show the presence of poly mineral clay. A glance at the intensity magnitude reveals a predominance of the quartz (Figure 9).

**Table 2. Chemical composition of the clay of Thicky**

SiO <sub>2</sub>	Al <sub>2</sub> O <sub>3</sub>	FeO <sub>3</sub>	CaO	MgO	Na <sub>2</sub> O	K <sub>2</sub> O	TiO <sub>2</sub>	PF	Total
61,10	19,4	5,15	0,75	0,95	0,55	1,85	0,85	7,21	98,01

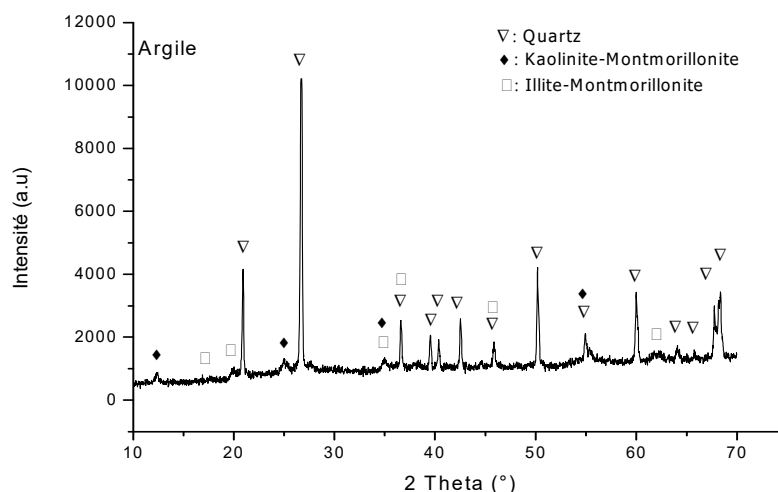


Fig. 9 . Clay diffractogram

#### 4 CHARACTERIZATION OF THE STUDIED AGGREGATES

We have studied, in this work, the natural and artificial aggregates. These aggregates are characterized by determining their bulk densities and absorption coefficients.

##### 4.1 AGGREGATES CHARACTERIZATION METHODS

##### 4.1.1 BULK DENSITY DETERMINATION

This parameter is essential in any study of the concrete because it allows us later to determine the amounts to use for each material present in the concrete. In this study, the bulk density determination was done with a pycnometer (Figure 10).



Fig. 10. Pycnometer filled with water

To achieve the test, a sample  $M$  of the material is weighed. After that, the sample is introduced in the pycnometer filled with water; the mass of the whole is recorded as  $M_1$ . The material is removed from the mixture and the mass of the pycnometer filled with water is named  $M_2$ . The following formula helps to find the bulk density:

$$\rho = \frac{M \times \rho_{eau}}{M_1 + M - M_2} \text{ [Eq. 1]}$$

#### 4.1.2 DETERMINATION OF THE ABSORPTION COEFFICIENT

Some granular materials can show an internal porosity that can be detrimental. In fact, the water inside the aggregate causes the spalling of the concrete when the latter is subjected to a low temperature for a long period.

The absorption coefficient is defined as the ratio of the increase of the sample's mass after inhibition in the water to the dry mass of the sample. This inhibition is achieved by immersing the sample in water for 24 hours at a 20°C room temperature [2].

The absorption coefficient is calculated as follows:

$$Abs = \frac{M_a - M_s}{M_s} \text{ [Eq. 2]}$$

where  $M_a$  represents the mass of the sample after immersion in water; and  $M_s$  the mass of the dry sample after passing through the heating chamber at 105°C.

#### 4.2 RESULTS OF THE AGGREGATES CHARACTERIZATION

##### 4.2.1 NATURAL AGGREGATES

The aggregates used in this study include the basalt, limestone and dune sand. They are natural aggregates for they have been extracted straight from nature and had not gone through any transformation but mechanical. In other words, the only transformations they must not experience to the risk of becoming artificial are those physical, chemical or even thermal.

The basalt (Figure 11) and the limestone (Figure 12) have a grain size class comprised between 8 and 16 mm. Limestone comes from Goundiane and the dune sand (Figure 13) from Kayar. The bulk density and the absorption coefficient about each type of aggregate have been determined (Table 3).



**Fig. 11 . Basalt**



**Fig. 12. Limestone**



**Fig. 13. Dune sand**

Table 3. Bulk density and absorption coefficient of natural aggregates

Material	$\rho_{eau}$ (Kg/m <sup>3</sup> )	$\rho$ (Kg/m <sup>3</sup> )	Abs (%)
Basalt	1	2.95	0.74
Limestone	1	2.51	3.77
Sand	1	2.55	1.19

4.2.2 ARTIFICIAL AGGREGATES

They have the same features as natural aggregates that have been underscored for fired clay aggregates at different temperatures. These features are summarized in Table 4.

Table 4. Bulk density and absorption coefficient of artificial aggregates

Matériau	$\rho_{eau}$ (Kg/m <sup>3</sup> )	$\rho$ (Kg/m <sup>3</sup> )	Abs (%)
Clay aggregates fired at 1100°C	1	2.28	10.4
Clay aggregates fired at 860°C	1	2.39	13.33

4.2.3 ANALYSIS AND INTERPRETATION OF RESULTS

The results achieved on aggregates allow to classify them into different categories and to plot their curve for a better assessment.

The basalt belongs to category A which is the most resistant, followed by the limestone which falls into the category B and the two clays into the category D because of their high absorption coefficient.

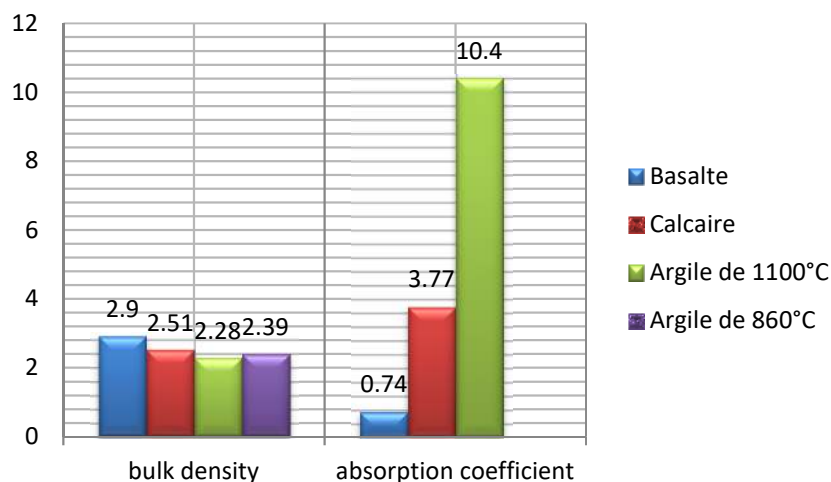


Fig. 14. Representation of the bulk density and the absorption coefficient

The figure 14 shows that the bulk density of the basalt is higher than those of other materials; it is followed by the clay fired at 860°C, then by limestone and finally by the clay fired at 1100°C. This means that the basalt is the heaviest material and clay fired at 1100°C the lightest.

Besides, the basalt absorption coefficient is extremely low; it is followed by the one of the limestone, then of the clay fired at 1100°C. The clay fired at 860°C does not have any absorption coefficient because some particles have been dissolved after a 24-hour-inhibition; its exploitation was so compromised that we were at risk of causing miscalculations.

According to these results, we can conclude that the firing temperature is not suitable for a durable material. This assessment has to be confirmed with other tests we achieved.

## 5 CHARACTERIZATION OF THE CONCRETE

### 5.1 FORMULATION OF THE CONCRETE

The formulation of the concrete was carried out with the Dreux GORISSE method in order to define the different proportions of the items that constitute each concrete.

The obtained results are presented in Table 5.

*Table 5. Proportions of the components of the different concretes*

Concrete	C/E	Ciment (Kg/m <sup>3</sup> )	Eau (L/m <sup>3</sup> )	Granulats utilisés (Kg/m <sup>3</sup> )	Sable (Kg/m <sup>3</sup> )
Basalt aggregate-based concrete	1,52	312,5	223,22	1361,42	633,67
Limestone aggregate-based concrete	1,52	312,5	256,81	1158,36	633,67
Clay aggregate-based concrete fired at 1100°C	1,52	312,5	322,57	1052,22	633,67
Clay aggregate-based concrete fired at 860°C	1,52	312,5	360,57	1102,98	633,67

### 5.2 CHARACTERISATION OF THE FRESH CONCRETE

The slump and bulk density of the fresh concrete have been determined.

#### 5.2.1 SLUMP

The slump test allows to examine the plasticity of the concrete but also to determine its consistency category. This factor has been established with the slump test cone (Figure 15).



*Fig. 2. Slump test cone*

To do the test, the formwork, as well as the bearing plate, has to be damped beforehand. Then, the formwork must be fixed on the bearing plate. After, we fill the formwork; at each 3 successive layers of the same height, we use the tapping rod and give 25 blows. When the formwork is full, the upper edge needs to be leveled by rolling the rod. At last, we lift the formwork cautiously and read the slump with a ruler.

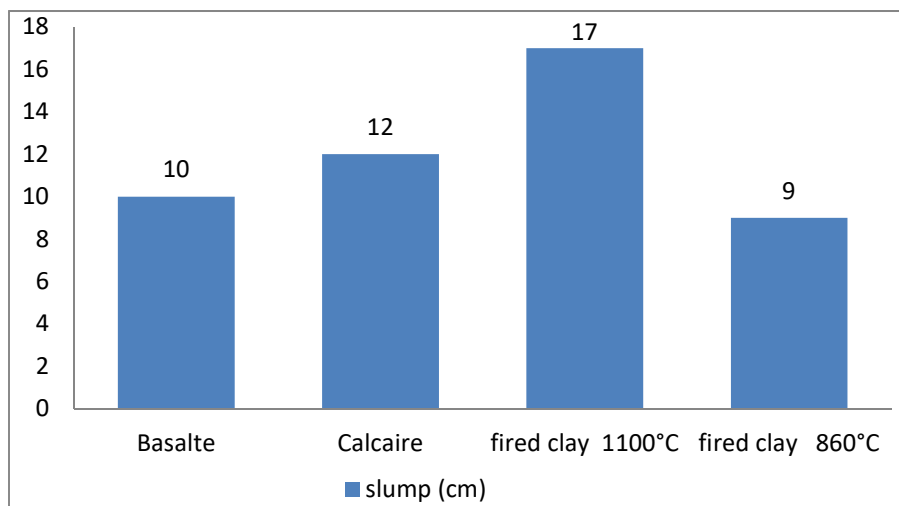


Fig. 16. Results of the slump

The figure 16 tells us about the consistency categories of each concrete. Hence, the basalt concrete and the limestone concrete are very plastic and belong to category S3. The clay aggregate-based concrete fired at 1100°C is a fluid concrete because of the significant amount of water, and belongs to category S4. In contrast, the clay aggregate-based concrete fired at 860°C should also be fluid because of the significant amount of water. But while processing, we noticed that the aggregates broke down inside the cement mixer. That increased the paste and thus improved the plasticity of the concrete.

### 5.2.2 BULK DENSITY

We had to determine the wet density of the concrete. For this purpose, we used formworks (Figure 17). These formworks are weighed first with wet concrete, then without the concrete.

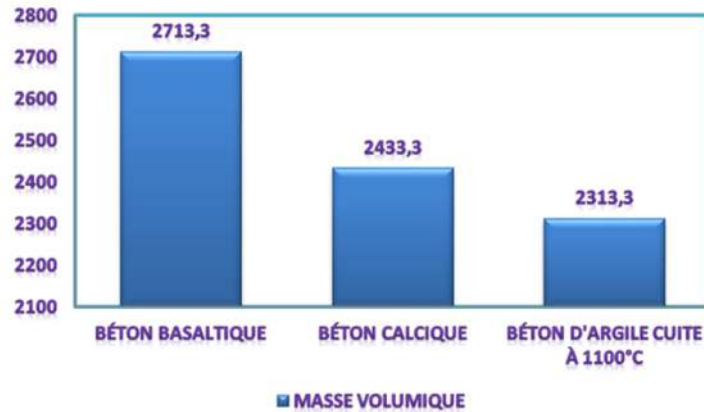


Fig. 17. Thermal formwork

Equation 3 is a method of calculating the bulk density of the concretes to use.

$$\rho = \frac{m}{v} \text{ [Eq. 3]}$$

Where  $\rho$  represents the bulk density of the concrete in  $\text{Kg.m}^{-3}$ ,  $m$  is the density of the wet concrete expressed in Kg and  $v$  is the volume of the formwork in  $\text{m}^3$ .



*Figure 18: Results of bulk density*

Figure 18 shows that the density of the basalt concrete is higher than those of the limestone concrete and the clay-based concrete. The latter is lighter due to expanded clay aggregates.

### 5.3 CHARACTERIZATION OF THE HARDENED CONCRETE

#### 5.3.1 THERMAL TEST

The test consists of determining the thermal conductivity along with the specific heat capacity of the concrete. Thus, we used the hot asymmetric plan with the rear side isolated. This apparatus is shown in Figure19:



*Figure 19: Apparatus of the hot asymmetric plan method*

A planar heating element called probe, as thick and large as the sample ( $10 \times 10 \text{ cm}^2$ ) is placed between this one and a polyurethane foam sample. A thermocouple made of two wires with diameters equal or below  $0.05 \text{ mm}$  is stuck on the surface of the element in connection with the polyurethane. The apparatus is completed with a block of polyurethane placed on top of the sample and the whole system is placed between two  $4 \text{ cm}$ -thick aluminium blocks. A level flow is applied to the probe and the evolution of the temperature  $T(t)$  of the thermocouple is registered. The data collected is saved in a computer as shown in figure 27, and then exported in the programming software MATLAB to calculate the thermal conductivity as well as the effusivity. The specific heat capacity of the concrete can be calculated thanks to these two sizes and the specific bulk density.

The thermal conductivity is the capacity of a material to transmit thermal energy, the higher it is, the more conducting the material is; and the lower it is, the more the material is insulating.

The thermal effusivity (Equation 4) determines the capacity of the material to absorb thermal energy. The higher the effusivity, the more the material absorbs energy without heating up considerably; and on the contrary, the lower it is, the faster the material heats up.

The specific heat capacity (Equation 5) of a body is equal to the quantity of heat to provide in order to raise by 1K the mass unit temperature. The higher it is, the less the body heats up.

$$E = \sqrt{\lambda\rho c} \text{ [Eq. 4]}$$

$$c = \frac{E^2}{\lambda\rho} \text{ [Eq. 5]}$$

Where E is the thermal effusivity in  $J.K^{-1}.m^{-2}.s^{-1/2}$ ;  $\lambda$  the thermal conductivity in  $W.m^{-1}.K^{-1}$ ;  $\rho$  the bulk density of the material in  $Kg.m^{-3}$  and c the specific heat capacity of the material in  $J.Kg^{-1}.K^{-1}$

The thermal tests are not performed on the clay fired at 860°C since the results of other tests prove that it does not have the satisfactory attributes for the concrete.

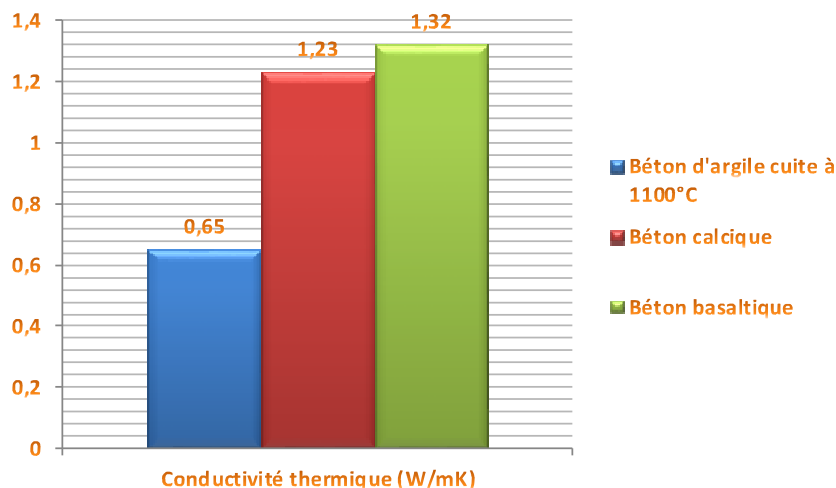


Fig. 20. Curves of the thermal conductivities of concretes

The figure 20 shows that the thermal conductivity of clay concrete is lower; it's followed by the limestone concrete. The basalt concrete has a higher conductivity, which means that the clay concrete is insulating and that other concretes are less insulating, therefore conducting.

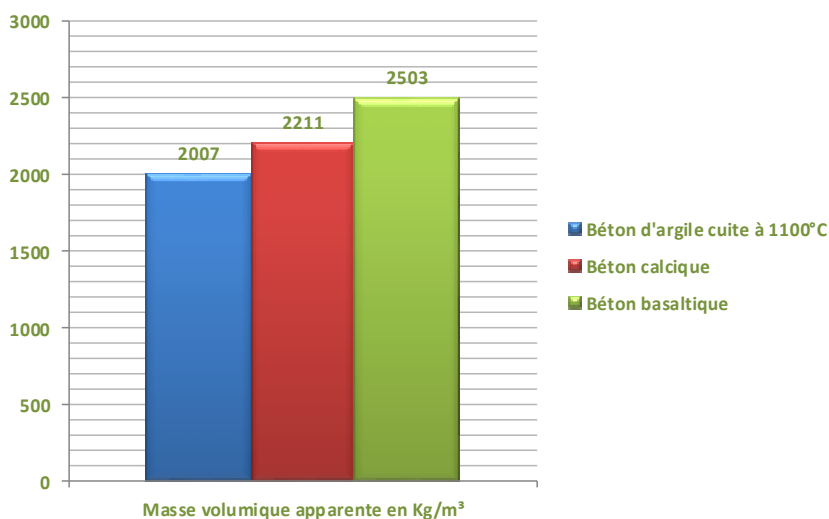
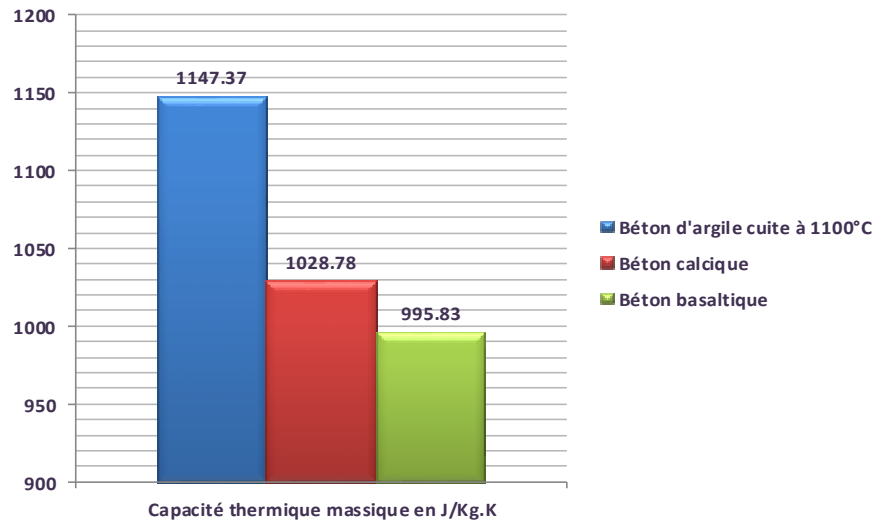


Fig. 21. Curves of the bulk specific density

Concerning the Figure 21, we can notice that the specific bulk density of the clay concrete fired at 1100°C is lower than other concretes, it is followed by the bulk density of the limestone concrete and finally by the basalt concrete which has the highest specific bulk density. Yet, when we compare these results with those obtained for the wet density, we have the same features except that there was water evaporation and that that specific bulk density is useful to calculate the thermal capacity of the concretes. The clay concrete fired at 1100°C is lighter than other concretes.



**Fig. 22. Curves of the specific heat capacity**

However, the figure 22 indicates that the thermal capacity of the clay concrete fired at 1100°C is higher than those of other concretes, it is followed by that of the limestone concrete and at last by that of the basalt concrete which has a lower thermal capacity. This means that it needs a significant amount of heat to raise the temperature of the concrete; therefore the clay concrete fired at 1100°C resists better to heat.

### 5.3.2 MECHANICAL TESTS

Mechanical tests performed on concretes are compression tests and splitting tensile tests.

The compression test of the concrete (Figure 23) allows to define the resistance of the concrete to compression. The test piece in study (16x 32 cm) undergoes an increasing load until it collapses. The resistance to the compression is the ratio of the breaking load and the cross-section of the test piece.

The splitting tensile test (Figure 24) permits to know the resistance of the concrete to tension. To do this test, a compressive stress along two opposite generators is applied to the test piece. This compressive stress leads to tension stress in the plane passing through these two generators. The breaking, due to these tension stresses, occurs in this plane. The calculation allows us to define the tension corresponding with that break.



Fig. 23. compression test



Fig. 24. splitting tensile test

The compression and splitting tensile test results made it possible to draw the following curves (Figures 25 and 26)

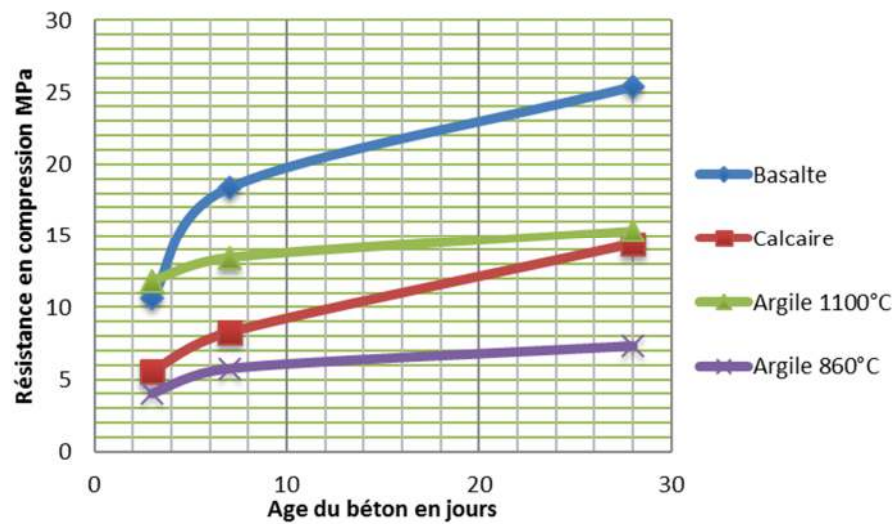
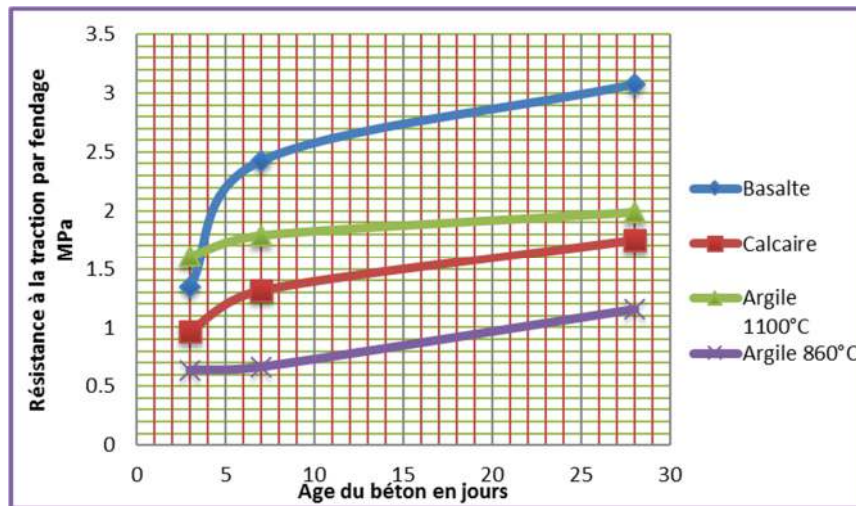


Fig. 25. Curve of the resistance in compression of the concrete according to age



**Fig. 26. Curve of the resistance in splitting tension of the concrete according to age**

Figure 25 illustrates that the resistance to compression of the clay aggregates-based concrete fired at 1100°C is much higher than resistances to compression of limestone concrete and clay concrete fired at 860°C. However, it is slightly higher than that of the basalt concrete. This means that the basalt concrete has observed a setting delay in comparison with the clay concrete fired at 1100°C.

From the 7<sup>th</sup> day up to the 28<sup>th</sup> day, the resistance of the basalt concrete is higher and it is followed by the clay concrete fired at 1100°C, then the limestone concrete. The clay concrete fired at 860°C has a lower resistance.

In a nutshell, the basalt concrete has a better resistance than the clay concrete fired at 1100°C. The clay concrete fired at 860°C has a poor resistance compared with other concretes and does not, consequently, fit construction.

Figure 26 presents almost the same features as figure 25.

At 3 days, the resistance to tension of the clay aggregates-based concrete fired at 1100°C is considerably higher than those of the basalt concrete, the limestone concrete and the clay concrete fired at 860°C.

From the 7<sup>th</sup> to the 28<sup>th</sup> day, the resistance to tension of the basalt concrete is higher and it is followed by the clay concrete fired at 1100°C, then by the limestone concrete. The clay concrete fired at 860°C has also a lower resistance in compression as for the tension. Though, the 7<sup>th</sup> day, we can notice a drop of the resistance to the tension of the clay concrete fired at 1100°C.

The basalt concrete has a better resistance to compression as well as to tension than all other concretes.

## 6 CONCLUSION

This study helped us make clay-based expanded aggregates from Senegal. The characteristics of these aggregates have been compared with those of common gravels. The use of these gravels has brought satisfactory results when they undergo the right transformation.

For the clay aggregates studied, the best firing temperature is 1100°C. However, for better results taking into account the absorption as well as the bulk density, other tests could be carried out with different temperatures above and under 1100°C. That will allow us to find the optimum temperature and the minimum one in order to obtain a stability of clay aggregates; then, the maximum temperature and finally, the firing limit temperature to check the total vitrification of the material.

We are looking forward the inclusion of this type of expanded clay in the factories of companies like SOFAMAC for a step forward in the construction sector and civil engineering works.

**REFERENCES**

- [1] Laukaitis A, Zurauskas R, Keriene J, 'The effect of foam polysterene aggregates on cement composite properties' cement and concrete composites, 27, P41-47, 2005
- [2] Saradhi babu D, Ganesh babu K, Wee t. H, 'Properties of lightweight expanded polystyrene aggregate concrete containing fly aash,' Cement and concrete Research, 35, P1218-1223, 2005
- [3] Milled K, Le roy R, Sab K, Boulay C, 'Compressive behavior of an an idealised eps lightweight concrete size effects and failure mode' Mechanics of materials, 36, P1031-1046, 2004
- [4] Wang H. Y, Tsai K. C, 'Engineering properties of lightweight aggregate concrete made from dresged silt, Cement and Concrete Composites' 28, P481-485, 2006
- [5] Yang C.C, Huang R, 'Approximation strength of lightweight aggregate using micromechanics method' advanced Cement Based Materials, 7, P133-138, 1998
- [6] Chi J. M, Huangg R, Yang C. C, Chang J. J 'Effect of aggregate properties on the strength and stiffness of lightweight concrete' Cement and Concrete Composites, 25, P197-205, 2003.